

## Inverse Compton Process in Quasars and Seyfert-Type Nuclei

Katsuo TAKARADA

*Department of Physics, Nagoya University, Nagoya*

(Received June 13, 1969)

The inverse Compton spectral power of the infrared source, which is optically thick to its own radiation due to the synchrotron self-absorption process, is calculated. A radio source of a single ensemble of relativistic electrons and magnetic fields is considered. These electrons emit synchrotron radiation, the high frequency part of the high frequency cutoff of which is observed in the infrared frequency range. A small fraction of the synchrotron photons suffers the inverse Compton scattering by the same ensemble of relativistic electrons. The scattered radiation is observed in the optical range. On the basis of this interpretation, the physical parameters of the infrared and optical source of 3C 273 are determined. A possible role played by the inverse Compton process is discussed for Seyfert-type nuclei.

### § 1. Introduction and summary

In recent years, much attention has been paid to the similarity between some of the quasars and some of the nuclei of Seyfert-type galaxies. A prominent feature of these objects is the enormous energy release in the infrared frequency range. Their output energy so far observed is mainly in this frequency range. Therefore, in order to clarify their structures, it is of prime importance to interpret the large infrared radiation.

Though the emission mechanism of the infrared radiation of the quasars and the Seyfert-type nuclei is not yet clear, the synchrotron mechanism is one of likely candidates. The possible presence of polarization in the infrared of 3C 273,<sup>1)</sup> though not confirmed, may support this mechanism. We assume the infrared radiation of quasars and Seyfert-type nuclei to be produced by the synchrotron mechanism. As for the size of infrared emitting region, the rapid time variation with the time scale of the order of one day observed for NGC 1068 and NGC 4151<sup>2)</sup> indicate the linear dimension of the order of  $10^{16}$  cm or less. In such a source with a large flux and a small dimension, the inverse Compton process may play a significant role.<sup>3)</sup>

In a previous paper<sup>3)</sup> (hereafter referred to as paper I), we have calculated the inverse Compton spectral power of the optically thin radio source and have interpreted the optical continuum radiation of quasars by the combination of the synchrotron and the inverse Compton processes. We have also shown a method by which source parameters can be determined. The conclusion was that the optical and radio emissions of the quasars originate from the same region of space and their spectra can be explained by a single ensemble of relativistic electrons.

According to recent radio observations, however, some radio sources associated with quasars or Seyfert-type nuclei have several components, each of which seems to be optically thick below some frequency. This frequency is higher, the dimension of the component is smaller.<sup>4)</sup> Sources of the infrared radiation seem also to become optically thick at a high frequency.<sup>1)</sup> Therefore, the conclusions and proposals made in paper I, where the radio sources are assumed to be optically thin, are not acceptable without appropriate modifications.

Under the assumption that the infrared radiations are produced by the synchrotron process, possible mechanisms to cause a low frequency cutoff are the free-free absorption due to thermal electrons, the low energy cutoff of relativistic electrons, the Tsytovich effect and the synchrotron self-absorption.<sup>5)</sup> Of these, the synchrotron self-absorption process may be most probable because of the large flux of radiation emitted within extremely small volume.<sup>6)</sup>

In the present paper, the inverse Compton spectral powers are calculated for infrared sources with a large optical depth due to the synchrotron self-absorption, and we interpret the optical continuum radiations of quasars and also obtain physical parameters of infrared sources based on our interpretation.

In § 2, we calculate the inverse Compton spectral power of an optically thick source which contains relativistic electrons of power index  $\beta$  and magnetic fields. In the frequency range where the inverse Compton power dominates the synchrotron power, the former has the frequency dependence of the form  $\nu^{(1-\beta)/2}$  over a sufficiently wide frequency range.

In § 3, an interpretation of the optical continuum as well as the infrared radiations of 3C 273 is given by the combination of the inverse Compton and the synchrotron processes as summarized below. The synchrotron radiation which becomes optically thick at somewhere in a frequency range between  $10^{11}$  c/s and  $10^{13}$  c/s due to the synchrotron self-absorption process and whose high frequency cutoff due to the upper cutoff of the relativistic electrons is about  $10^{13}$  c/s suffers the inverse Compton scattering by the same ensemble of relativistic electrons as those responsible for the synchrotron radiation. If we assume  $\beta=1$ , the infrared and the optical continuum radiations can be interpreted by the single ensemble of relativistic electrons. On the basis of this interpretation, we determine physical parameters of the source. The optical continuum radiations of some of the quasars which have two components, one of which shows steep increase with decreasing frequency in the lower frequency range and the other of which shows rather flat slope in the higher frequency range may essentially be interpreted in a similar manner.

In § 4, comments on the nuclei of Seyfert-type galaxies, NGC 4151 and 3C 120, are made. The inverse Compton power of the infrared source of NGC 4151 is sufficiently high, and it may energetically be the source of excitation of the gas which is producing emission lines. In particular, the very hot gas to produce coronal lines considered by Oke and Sargent<sup>7)</sup> may not necessarily be

required if the inverse Compton photons are available. The large infrared flux<sup>1)</sup> and the flat component of the optical continuum in the higher frequency range of 3C 120<sup>8)</sup> is interpreted in the same way as in 3C 273. Conclusions and discussion are made in § 5.

### § 2. Inverse Compton spectral power from optically thick source

We consider a uniform sphere of radius  $R$ , which contains relativistic electrons and magnetic fields of strength  $H$ . We assume that an acceleration mechanism of particles is operating throughout the source and, as a result, the source is in a stationary state.

#### 1) Synchrotron spectral power

Let the energy distribution of relativistic electrons be given by the power-law,

$$N(\gamma) d\gamma = \begin{cases} N_0 \gamma^{-\beta} d\gamma & \text{for } \gamma_2 \geq \gamma \geq \gamma_1 (\gg 1), \\ 0 & \text{for otherwise,} \end{cases} \quad (1)$$

where  $\gamma = E/mc^2$ . As the isotropic volume emissivity of synchrotron radiation we use the following approximation,<sup>9)</sup>

$$p_s(\nu) d\nu = b(\beta) \frac{e^3}{mc^2} \left( \frac{3e}{4\pi mc} \right)^{(\beta-1)/2} H^{(\beta+1)/2} N_0 \nu^{(1-\beta)/2} d\nu, \quad (2)$$

where  $b(\beta) = 4.77(0.29)^{(\beta-1)/2}$ ,\*)  $H^{(\beta+1)/2}$  is an average value of this quantity in the radiating region, and Eq. (2) is, in the present approximation, restricted within the frequency range,

$$\nu_2 \left( = 0.29 \times \frac{3eH}{4\pi mc} \gamma_2^2 \right) \geq \nu \geq \nu_1 \left( = 0.29 \times \frac{3eH}{4\pi mc} \gamma_1^2 \right).$$

The synchrotron absorption coefficient is given by<sup>9)</sup>

$$\mu(\nu) = g(\beta) \frac{e^3}{2\pi m^2 c^2} \left( \frac{3e}{2\pi mc} \right)^{\beta/2} H^{(\beta+2)/2} \nu^{-(\beta+4)/2} N_0, \quad (3)$$

where  $g(\beta)$  is numerical constant of the order of unity. The values of  $g(\beta)$  and  $b(\beta)$  are shown for several values of  $\beta$  in Table I.

Table I.

β	0.5	1.0	1.5	2.0	2.5	3.0
<i>b</i> (β)	6.50	4.77	3.50	2.57	1.89	1.38
<i>g</i> (β)	1.32	0.96	0.79	0.70	0.66	0.65

\*) The expression for  $b(\beta)$  in paper I, i.e.  $b(\beta) = 4\pi(0.29)^{(1-\beta)/2}$  should be replaced by the expression given above. However, numerical results in paper I have been obtained by using the correct expression.

Let the frequency which satisfies the relation  $\mu(\nu)R=1$  be denoted by  $\nu_{\max}$ . Equation (3) can be applied only to the frequencies far less than  $\nu_2$  and we restrict ourselves to the case,  $\nu_{\max} \ll \nu_2$ . For  $\nu \gg \nu_{\max}$ , the source is optically thin. In this case, the spectral power of the synchrotron radiation emitted from the source is  $P_s(\nu) d\nu = (4\pi/3)R^3 p_s(\nu) d\nu$ . For  $\nu \ll \nu_{\max}$ , the source is optically thick. Then, the synchrotron spectral power of the source is given by  $P_s(\nu) d\nu = 4\pi R^2 p_s(\nu) \times d\nu/\mu(\nu)$ . For the intermediate frequency range, we use an expression which is derived by the elementary consideration that the path-length of a photon with  $\nu$  is, on an average,  $1/\mu(\nu)$  and whether it can escape from the source or not depends on the position and on the direction of emission. From this we obtain  $p_s(\nu) d\nu = (11/12)\pi R^3 p_s(\nu) d\nu$  for  $\nu = \nu_{\max}$ . Consequently, we have the following expressions,

$$\frac{P_s(\nu) d\nu}{(4\pi/3)R^3} = \begin{cases} p_s(\nu) d\nu & \text{for } \nu \gg \nu_{\max}, \\ 3p_s(\nu) (\nu/\nu_{\max})^{(\beta+4)/2} d\nu & \text{for } \nu \ll \nu_{\max}, \\ \frac{11}{16} p_s(\nu) d\nu & \text{for } \nu = \nu_{\max}. \end{cases} \quad (4)$$

## 2) Number density of the synchrotron photons

The number density of the synchrotron photons in the optically thin frequency range is obtained as in paper I,

$$n_s(\nu) d\nu = \frac{R}{c} \cdot \frac{p_s(\nu)}{h\nu} d\nu \quad \text{for } \nu > \nu_{\max}.$$

In the case of optically thick frequency, the number density is estimated as follows.

Consider a length  $r (\ll R)$ , for which  $\mu(\nu)r=1$  holds. In the sphere of radius  $R$ , we consider a small sphere whose radius is  $r$  and whose center is at

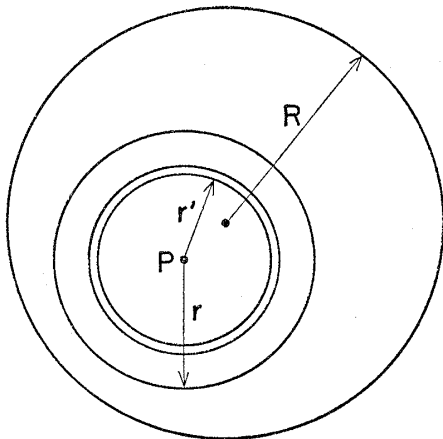


Fig. 1.

a point  $P$ . The number density of the synchrotron photons at a point  $P$  is determined by the photons which are emitted within the small sphere of radius  $r$ , since the photons from the outer part of the small sphere are, on an average, absorbed before they arrive at  $P$ . The flux at  $P$  due to the photons emitted in a unit volume at a distance  $r'$  from  $P$  is  $(p_s(\nu)/h\nu)/4\pi r'^2$ . Therefore, the flux at  $P$  due to the photons emitted in the shell of radius  $r'$  is  $dI(\nu) = p_s(\nu) \times dr'/h\nu$ . Taking into account the contribution from the entire sphere of radius  $r$ , we obtain, as the flux at  $P$ ,

$$I(\nu) = \frac{p_s(\nu)}{h\nu} r = \frac{p_s(\nu)}{h\nu} \cdot \frac{1}{\mu(\nu)}.$$

The number density is accordingly given by

$$n_s(\nu) d\nu = \frac{1}{c\mu(\nu)} \cdot \frac{p_s(\nu)}{h\nu} d\nu \quad \text{for } \nu \ll \nu_{\max}. \quad (5)$$

This result can be understood also by considering that the small sphere of radius  $r$  is uniform and optically thin, and the average time for photons to escape from this sphere is of the order of  $r/c$ . Assuming Eq. (5) to be valid for  $\nu = \nu_{\max}$ , and rewriting  $p_s(\nu)$  and  $\mu(\nu)$  with Eqs. (2) and (3), we get the number density of the synchrotron photons as follows,

$$n_s(\nu) d\nu = \begin{cases} n_0(\beta) \nu^{-(\beta+1)/2} d\nu & \text{for } \nu \geq \nu_{\max}, \\ n_0(\beta) \nu_{\max}^{-(\beta+4)/2} \nu^{3/2} d\nu & \text{for } \nu \leq \nu_{\max}, \end{cases} \quad (6)$$

where

$$n_0(\beta) = \frac{R}{hc} \cdot \frac{e^3}{mc^2} b(\beta) \left( \frac{3e}{4\pi mc} \right)^{(\beta-1)/2} H^{(\beta+1)/2} N_0.$$

For the frequency range  $\nu \gg \nu_{\max}$ , Eq. (6) is a good approximation for the whole region of the source. For  $\nu \ll \nu_{\max}$ , it is a good approximation in the innermost region, but near the surface of the source, it gives over-estimation. For the frequencies nearly equal to  $\nu_{\max}$ , Eq. (6) does not give a good approximation. However, since the number of photons with frequencies nearly equal to  $\nu_{\max}$  is small compared with the total number of the synchrotron photons because of the high-power dependence of the absorption coefficient on frequency, it is unlikely that Eq. (6) produces a serious error in the spectrum of the inverse Compton power to be calculated.

### 3) Inverse Compton spectral power

For the energy of synchrotron photons and relativistic electrons, we apply the condition,  $\gamma \cdot h\nu \ll mc^2$ ,<sup>9),10)</sup> under which the energy differential cross section for the inverse Compton process is given by<sup>11),12)</sup>

$$\sigma(\nu', \nu, \gamma) = \frac{2\pi r_e^2}{\gamma^2} \left[ 1 + \frac{\nu'}{4\gamma^2\nu} - 2 \left( \frac{\nu'}{4\gamma^2\nu} \right)^2 + 2 \frac{\nu'}{4\gamma^2\nu} \ln \left( \frac{\nu'}{4\gamma^2\nu} \right) \right], \quad (7)$$

where,  $\nu$  and  $\nu'$  are the frequencies of initial (synchrotron) and scattered (inverse Compton) photons, respectively, and  $r_e$  is the classical electron radius. The energy of scattered photons is restricted within the range  $\nu \leq \nu' \leq 4\nu\gamma^2$ .

From Eqs. (1), (6) and (7), the production rate and the spectral power of the inverse Compton photons per unit volume can be calculated as

$$n_c(\nu') = c \iint N(\gamma) n_s(\nu) \sigma(\nu', \nu, \gamma) d\gamma d\nu$$

and

$$p_c(\nu') d\nu' = n_c(\nu') h\nu' d\nu'.$$

Depending on the values of  $\nu'$  and  $\nu_{\max}$ , the integrations must be effected for various ranges. We can explicitly obtain expressions for  $n_c(\nu')$  or  $p_c(\nu')$  after tedious integrations, however, they are so lengthy that we give results for various parameters in the figures. (For the procedure of calculation, see the Appendix.)

In our calculation, the values of  $\nu_{\max}$ ,  $\gamma_1$ ,  $\gamma_2$ ,  $H$  and  $\beta$  are specified, then  $N_0$  and  $R$  are treated as free parameters. However, it must be remarked that the value of  $N_0$  and  $R$  are not independent of each other but have to satisfy the relation  $\mu(\nu_{\max})R=1$ .

For  $\nu' \gg \nu_{\max}$ , the inverse Compton spectral power of the entire source is given by  $P_c(\nu') d\nu' = (4\pi/3)R^3 p_c(\nu') d\nu'$ . Though we must take into account the synchrotron self-absorption process to obtain  $P_c(\nu') d\nu'$  for  $\nu \lesssim \nu_{\max}$ , it is of no meaning to do this because  $P_s(\nu) d\nu$  dominates  $P_c(\nu') d\nu'$  in this frequency range (see Fig. 2).

#### 4) Numerical results

In Fig. 2, the inverse Compton spectral powers per unit volume normalized by  $RN_0^2$  of partially thick sources are shown for several values of  $\beta$ . The other source parameters are  $H=1$  gauss,  $\gamma_2=10^4$ ,  $\gamma_1=5$  and  $\nu_{\max}=10^{-2}\nu_2$ . In the frequency range where the inverse Compton spectral power  $P_c(\nu') d\nu'$  (hereafter we will drop out primes if not necessary) dominates the synchrotron spectral power,  $P_c(\nu) d\nu$  has the  $\nu$ -dependence of the form,  $\nu^{(1-\beta)/2}$ , for a sufficiently wide frequency range. This result has been obtained in the case of optically thin source and is explained by the same reasoning as that given in paper I, namely, by the fact that the inverse Compton spectral power of a single electron,  $p_c(\nu, \gamma)$ , has the energy dependence,  $P_c(\nu, \gamma) \propto \gamma^2$  and can be approximated as  $p_c(\nu, \gamma) = p_c(\gamma) \delta(\nu - \nu_{cr})$ . Of course, the result is unchanged if parameters other than  $\beta$  are changed. In the figure, are also shown the synchrotron spectral powers normalized by  $N_0$  and divided by source's volume for the same parameters, which are obtained by using Eq. (4) in the present paper and Eq. (2) in paper I. Note that the parameters  $N_0$  and  $R$  are not independent as was stated previously but must satisfy the following relation,

$$\frac{1}{N_0^2 R} = 5.77 \times 10^8 (8.40 \times 10^6)^\beta \{g(\beta)\}^2 HR \nu_{\max}^{-(\beta+4)}.$$

We have no information on the value of  $\gamma_1$  observationally as well as theoretically. But under the present condition  $\nu_{\max} \ll \nu_2$ ,  $P_c(\nu) d\nu$  is not significantly affected by  $\gamma_1$  as seen from Fig. 3. In Fig. 4, the  $P_c(\nu) d\nu$ 's are shown for several  $\gamma_2$ 's. The cutoff frequency of  $P_c(\nu) d\nu$  is  $4\nu_2 \gamma_2^2 = 4.8 \times 10^6 \cdot H \gamma_2^4$ . For later reference, we present  $P_c(\nu)$ 's for various  $\nu_{\max}$ 's in Fig. 5. For fixed  $\nu_{\max}$ ,  $P_c(\nu)$

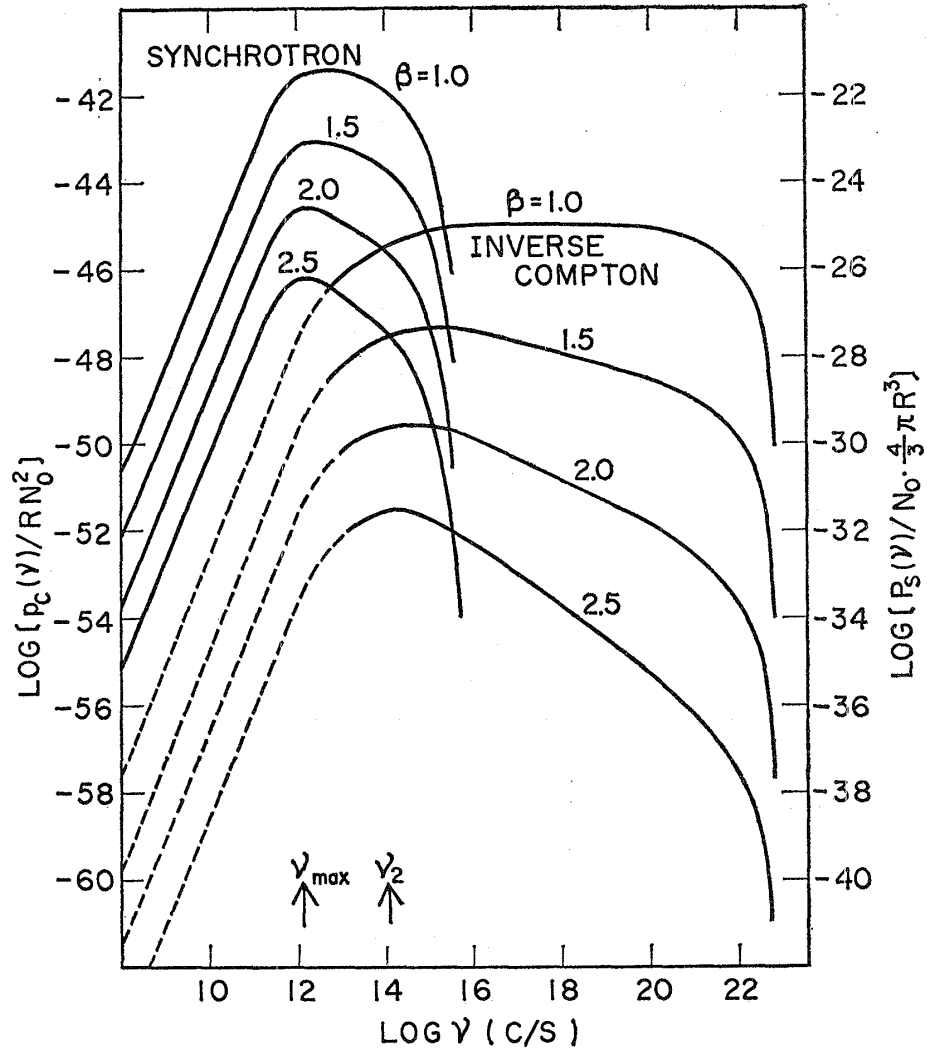


Fig. 2. The inverse Compton spectral powers per unit volume normalized by  $RN_0^2$  of optically thick sources are shown for several values of  $\beta$ . The other source parameters are  $H=1$  gauss,  $\gamma_2=10^4$ ,  $\gamma_1=5$  and  $\nu_{\max}=10^{-2}\nu_2$ . In the figure are also shown the synchrotron spectral powers of the source normalized by  $N_0$  and divided by source's volume for the same parameters. The left and right ordinates are for the inverse Compton and the synchrotron spectral powers in C.G.S. unit, respectively. The abscissa is frequency in cycle per second. These ordinates and abscissa are common to figures from 2 to 5.

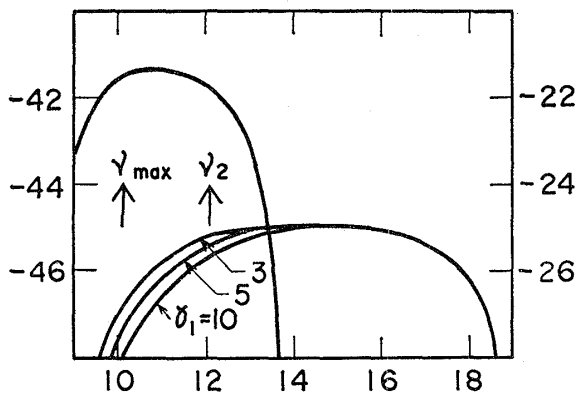


Fig. 3. The behaviours of the inverse Compton spectral powers for the different values of  $\gamma_1$  are shown. The other parameters are  $H=1$  gauss,  $\gamma_2=10^3$ ,  $\beta=1$  and  $\nu_{\max}=10^{-2}\nu_2$ .

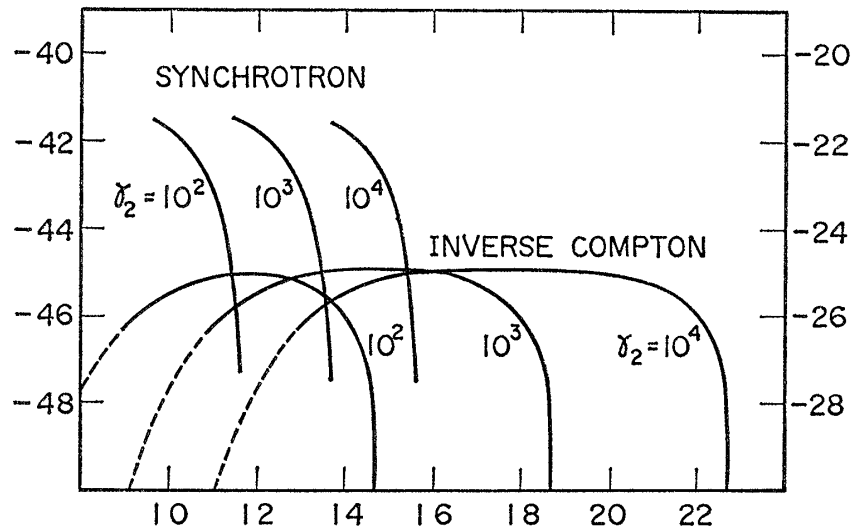


Fig 4 The behaviours of the inverse Compton spectral powers for the different values of  $\gamma_2$  are shown. The other parameters are  $H=1$  gauss,  $\gamma_1=5$ ,  $\beta=1$  and  $\nu_{\max}=10^{-2}\nu_2$

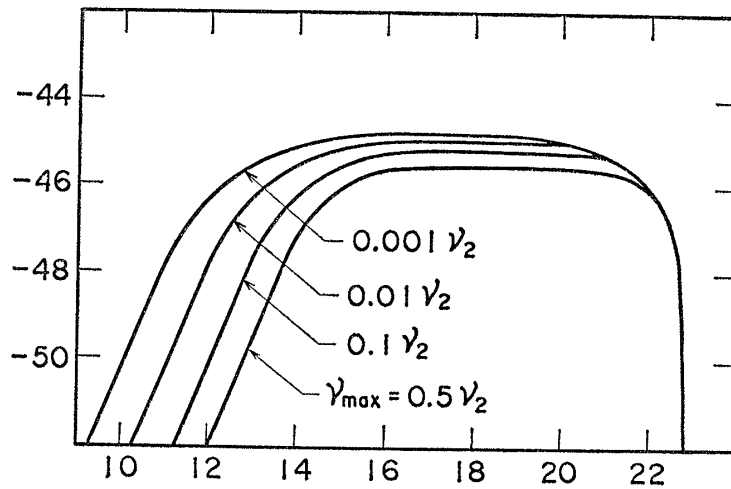


Fig 5 The inverse Compton spectral powers are shown for various values of  $\nu_{\max}$ . The other parameters are  $H=1$  gauss,  $\gamma_2=10^4$ ,  $\gamma_1=5$  and  $\beta=1$

has essentially the  $H$ -dependence of the form  $H^{(\beta+1)/2}$  so that we can easily obtain the value of  $P_c(\nu)$  for an arbitrary value of  $H$  from the figures

### § 3. Quasar 3C 273

#### 1) Interpretation of the infrared and optical continuum radiation

The flat continuum spectrum in nearly the whole optical range increases with decreasing frequency in the red<sup>13)</sup> and further increases steeply in the infrared range<sup>2),14)</sup>. This infrared spectrum with steep slope, which is shown in Fig 6, can be approximated by either a power-law or an exponential-law spectrum



within the range of observational error. If we take a steep power-law, the spectral shape of the resultant inverse Compton power is also a steep power-law as was shown in Fig. 2. Therefore, the flat spectrum of optical continuum cannot be explained in the spectral shape by the inverse Compton process, but must be explained by another ensemble of relativistic electrons or by some mechanism other than the synchrotron and the inverse Compton. On the contrary, if we take an exponential-law spectrum, or if we regard the infrared spectrum as a high frequency part of the high frequency cutoff of the synchrotron radiation and assume  $\beta=1$ , the flat optical continuum can be explained by the inverse Compton process in so far as spectral shape is concerned.

Though we have only poor knowledge of the acceleration mechanism expected operating in compact radio sources such as quasars and Seyfert-type nuclei, it seems unlikely for us that two different ensembles of relativistic electrons, the one responsible for the infrared emission and the other responsible for the optical emission, are produced in quite a small region of space. The radio spectra of small components found in the compact radio sources often appear to have flat spectra.<sup>15)</sup>

With these two reasons, we assume that the index  $\beta$  of the relativistic electrons responsible for the infrared emission is unity and interpret the optical continuum of 3C 273 to be produced by the inverse Compton process of the same ensemble of relativistic electrons as those responsible for the infrared emission.

## 2) Determination of physical parameters of radio source

Comparing the observed flux densities in the infrared spectral range with the synchrotron spectral power, we can estimate  $\nu_2 \simeq 10^{13}$  c/s as the high frequency cutoff of the synchrotron radiation, and  $f \simeq 2.5 \times 10^{-22}$  erg cm<sup>-2</sup> sec<sup>-1</sup> (c/s)<sup>-1</sup> as the flux density in the flat spectral range (see Fig. 6). The flux density of the flat optical continuum observed is about  $2.5 \times 10^{-25}$  ergs cm<sup>-2</sup> sec<sup>-1</sup> (c/s)<sup>-1</sup>.

To calculate the inverse Compton spectral power, it is necessary to specify the value of  $\nu_{\max}$ . Observations carried out so far, however, do not tell us the value definitely. In the frequency range between about  $10^{10}$  c/s (centimeter) and about  $10^{11}$  c/s (millimeter), the radio fluxes show large time variations (Dent,<sup>16)</sup> Epstein,<sup>17)</sup> Low<sup>18)</sup>). On the other hand, the infrared spectrum does not show the corresponding variation.<sup>18)</sup> Moreover, the recent radio observations reveal that the object consists of multiple sources in the radio frequency range and each

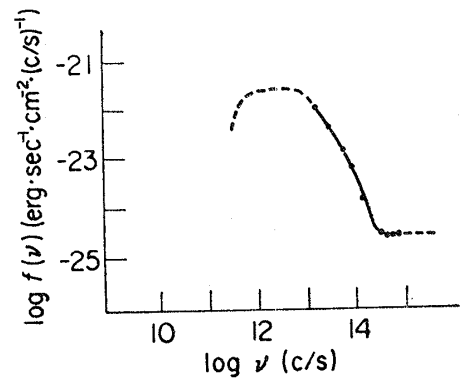


Fig. 6. The observed continuum spectrum of 3C 273 in the infrared and the optical range, which is taken from the paper by Pacholczyk and Weymann.<sup>2)</sup>

source is optically thick below some critical frequency.<sup>4)</sup> This critical frequency is higher, the dimension of the component is smaller. The infrared spectra of Seyfert nuclei reported by Low and Kleimann<sup>1)</sup> all seem to be optically thick in the range from about  $10^{10}$  c/s to about  $10^{11}$  c/s. These observational results show that the infrared spectrum does not extend, with the comparable level of flux density, to the millimeter and centimeter range, so that the infrared spectrum of 3C 273 is probably optically thick in the range between about  $10^{11}$  c/s and about  $10^{12}$  c/s.

The difference between the  $p_c(\nu)$ 's calculated for  $\nu_{\max} = 10^{11}$  c/s and  $\nu_{\max} = 10^{12}$  c/s is negligible in the present treatment which involves various approximations, as clearly seen from Fig. 5, and we use  $\nu_{\max} = 10^{11}$  c/s for the calculation of  $p_c(\nu)$ 's.

Using the observed and estimated fluxes and the relation  $4\pi D^2 f(\nu) = P(\nu)$ , we have

$$R^3 N_0 H \simeq 2.3 \times 10^{54}$$

from the synchrotron and

$$R^4 N_0^2 H \simeq 1.3 \times 10^{75}$$

from the inverse Compton spectral power. From these two relations we cannot determine  $R$ ,  $N_0$  and  $H$  uniquely, but can determine, for example,  $R$  and  $N_0$  as functions of  $H$ . In Table II, the values thus determined are shown with other quantities. In the Table,  $N$  is the number density of relativistic electrons and  $\tau_e(\gamma_2)$  is the life-time of the most energetic electrons. The last column is the ratio of the total energies of the relativistic electrons to magnetic fields.

Compared with the case of the optically thin source, the synchrotron self-absorption process results in decreases of the number density of the synchrotron photons per unit frequency range in lower frequency range. However, the amount of decrease in the integrated number density of the synchrotron photons over entire frequency range is small under the restriction  $\nu_{\max} \ll \nu_2$  so that the values in Table II are not essentially different from those of the optically thin source.<sup>3)</sup>

As was stated in paper I, the observation of X-ray flux,<sup>10)</sup> though not confirmed, indicates the presence of strong magnetic fields of the order of 100 gauss.

Table II.

$H$ (gauss)	$R$ (cm)	$N$ ( $\text{cm}^{-3}$ )	$\nu_{\max}$ (c/s)	$\tau_e(\gamma_2)$ (sec)	$W_e/W_H$
100	$6.2 \times 10^{15}$	$3.9 \times 10^5$	$4.0 \times 10^{12}$	$2.1 \times 10$	$5.6 \times 10^{-2}$
10	$2.0 \times 10^{16}$	$1.6 \times 10^5$	$1.1 \times 10^{12}$	$6.5 \times 10$	5.6
1	$6.2 \times 10^{16}$	$6.4 \times 10^4$	$2.8 \times 10^{11}$	$2.1 \times 10^2$	$5.6 \times 10^2$
0.1	$2.0 \times 10^{17}$	$2.3 \times 10^4$	$6.9 \times 10^{10}$	$6.5 \times 10^2$	$5.6 \times 10^4$

If we admit this value of the magnetic field, the source of the infrared and optical emission of 3C 273 has in order of magnitude the parameters given by the first row in Table II.

### 3) Comment on other quasars

The optical continuum spectra of the quasars, 3C 446 and 3C 279, consist of two components. The one shows steep increases of fluxes with decreasing frequency in the lower frequency range in  $\log f(\nu)$ - $\log \nu$  plot and the other has a flat spectrum in the higher frequency range (Oke<sup>20</sup>). The interpretation of these spectra is essentially the same as that of 3C 273. However, since the infrared observations are not available, we cannot give the quantitative treatment. If we take into account the self-absorption process, that is to say, if we consider the infrared source instead of the radio source, the argument given in paper I that the spectral shape of the optical continuum may be classified into three groups due to the position of the critical frequency at which  $P_c(\nu)$  becomes equal to  $P_s(\nu)$  may be regarded as a plausible interpretation.

## § 4. Comments on the nuclei of Seyfert-type galaxies, NGC 4151 and 3C 120

### 1) NGC 4151

The infrared observations were made by Low and Kleinmann<sup>1)</sup> and by Pacholczyk and Weymann.<sup>2)</sup> If we assume the infrared radiation to be produced by the synchrotron mechanism and assume  $\beta=1$  as in the case of 3C 273, we can regard the infrared flux as the higher frequency part of the high frequency cutoff of the synchrotron radiation and obtain  $\nu_2 \simeq 10^{13}$  c/s. The observed spectrum of NGC 4151 is shown in Fig. 7. The low frequency cutoff,  $\nu_{\max}$ , seems to be in the range from  $10^{11}$  c/s to  $10^{12}$  c/s.<sup>1)</sup> The flux density which is assumed nearly flat between  $\nu_{\max}$  and  $\nu_2$  is estimated as  $f_s(\nu) \simeq 10^{-21}$  ergs  $\text{cm}^{-2}$   $\text{sec}^{-1}$  (c/s)<sup>-1</sup> and we obtain  $P_s(\nu) = 4\pi D^2 f_s(\nu) \simeq 10^{31}$  erg  $\text{sec}^{-1}$  (c/s)<sup>-1</sup> where we have used  $D=10M_{\text{pc}}$ .<sup>7)</sup> The non-thermal optical continuum spectrum was obtained by Oke and Sargent,<sup>7)</sup> who determined the shape to be an exponential-law which cannot be attributed to the continuation from the infrared spectrum. Accordingly, if we admit the shape determined by Oke and Sargent, the emission mechanism of the non-thermal optical continuum of NGC 4151 is independent of the infrared emission. In any way, the optical continuum cannot be explained by the inverse Compton process of the infrared source so that the inverse Compton spectral power of the infrared source must be lower than the observed spectral power in the whole optical range,  $P_c(\nu) < 3 \times 10^{27}$  erg  $\text{sec}^{-1}$  (c/s)<sup>-1</sup>.

As for the size of the infrared emitting region, the rapid time variation of the order of one day,<sup>2)</sup> though it must be confirmed by further observations, indicates  $10^{16}$  cm or less. For the two cases of  $R=10^{16}$  cm and  $R=5 \times 10^{15}$  cm, we present the source parameters determined by taking  $H$  as a free parameter.

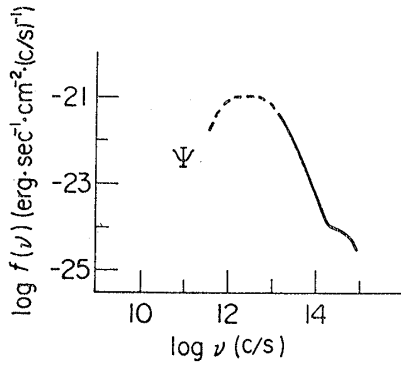


Fig. 7. The observed infrared and the non-thermal optical continuum spectra of NGC 4151, which are taken from the paper by Low and Kleinmann.<sup>1)</sup>

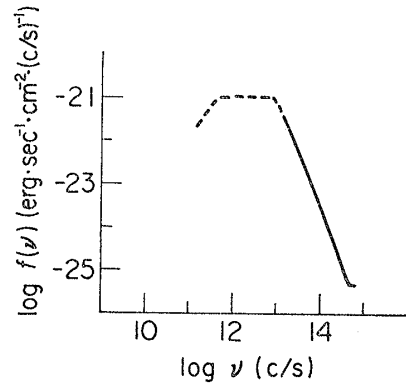


Fig. 8. The observed continuum spectrum of 3C 120 in the infrared and the optical range, which is taken from the paper by Low and Kleinmann.<sup>1)</sup>

Table III.

$H$	$r_2$	$R=5 \times 10^{15}$ cm			$R=10^{16}$ cm		
		$N_0$	$\log \nu_{\max}$	$P_c(\nu)$	$N_0$	$\log \nu_{\max}$	$P_c(\nu)$
$10^{-4}$	$2.9 \times 10^5$	$3.0 \times 10^3$	10.40	$2.4 \times 10^{31}$	$3.7 \times 10^7$	10.16	$5.7 \times 10^{30}$
$10^{-3}$	$9.2 \times 10^4$	$3.0 \times 10^7$	10.60	$2.4 \times 10^{30}$	$3.7 \times 10^6$	10.36	$5.7 \times 10^{29}$
$10^{-2}$	$2.9 \times 10^4$	$3.0 \times 10^6$	10.80	$2.4 \times 10^{29}$	$3.7 \times 10^5$	10.56	$5.7 \times 10^{28}$
$10^{-1}$	$9.2 \times 10^3$	$3.0 \times 10^5$	11.00	$2.4 \times 10^{28}$	$3.7 \times 10^4$	10.76	$5.7 \times 10^{27}$
1	$2.9 \times 10^3$	$3.0 \times 10^4$	11.20	$2.4 \times 10^{27}$	$3.7 \times 10^3$	10.96	$5.7 \times 10^{26}$
10	$9.2 \times 10^2$	$3.0 \times 10^3$	11.40	$2.4 \times 10^{26}$	$3.7 \times 10^2$	11.16	$5.7 \times 10^{25}$
$10^2$	$2.9 \times 10^2$	$3.0 \times 10^2$	11.60	$2.4 \times 10^{25}$	$3.7 \times 10$	11.36	$5.7 \times 10^{24}$

From Table III, we find that the restriction,  $10^{11}$  c/s  $< \nu_{\max} < 10^{12}$  c/s, is consistent with the condition  $P_c(\nu) < 3 \times 10^{27}$  erg sec<sup>-1</sup>(c/s)<sup>-1</sup> and we can exclude the cases of  $H=10^{-4}$ ,  $10^{-3}$ ,  $10^{-2}$  and  $10^{-1}$  gauss for both  $R$ 's.

According to Oke and Sargent,<sup>7)</sup> the optical continuum radiation extrapolated below the Lyman limit, which is capable of ionizing hydrogen, is  $1.1 \times 10^{40}$  erg sec<sup>-1</sup>. This is insufficient by about a factor of  $10^3$  to heat the gas which produces emission lines. If we assume that the total power of the inverse Compton process of the infrared source, which is approximately given by  $4\nu_2\gamma_2^2 \cdot P_c(\nu)$ , can heat the gas, it is energetically possible that the inverse Compton power is the source of heating the gas. In particular, to produce the coronal lines the hot gas is not necessarily required if the inverse Compton power is available.

## 2) 3C 120

The infrared observation was made by Low and Kleinmann,<sup>1)</sup> from which we obtain  $\nu_2 \simeq 10^{13}$  c/s and  $10^{11}$  c/s  $\lesssim \nu_{\max} < 10^{12}$  c/s. (See Fig. 8.) As the flux density in the range between  $\nu_2$  and  $\nu_{\max}$ , we have estimated  $f_s(\nu) \simeq 10^{-21}$  erg

$\text{sec}^{-1} \text{cm}^{-2} (\text{c/s})^{-1}$  by extrapolation of the observed spectrum. The output energy in the infrared amounts to the order of  $10^{46} \text{ erg sec}^{-1}$ . The optical continuum spectrum obtained by Oke, Sargent, Neugebauer and Becklin<sup>8)</sup> is nearly flat in the higher and is increasing with decreasing frequency in the lower optical range. The flux density of the optical continuum in the flat part is about  $f_c(\nu) \simeq 4 \times 10^{-26} \text{ erg cm}^{-2} \text{sec}^{-1} (\text{c/s})^{-1}$ . The optical time variation reported by Kinmann<sup>23)</sup> indicates  $R \simeq 3 \times 10^{16} \text{ cm}$  as the size of emitting region of the optical continuum. If we assume that the infrared continuum comes from the same region of space as that of the optical continuum and that the flat part of the optical continuum is produced by the inverse Compton process in the infrared source, then we can determine the source parameters as follows.

From the infrared flux we have

$$4\pi D^2 f_s(\nu) = P_s(\nu) = \frac{4}{3} \pi R^3 \times 6.44 \times 10^{-22} H N_0,$$

where the distance of 3C 120,  $D = 2.7 \times 10^{26} \text{ cm}$ . From the optical flux of the flat part, we have

$$4\pi D^2 f_c(\nu) = P_c(\nu) = \frac{4}{3} \pi R^3 \times 10^{-45} R N_0^2 H.$$

Substituting the values of  $R$ ,  $f_s(\nu)$  and  $f_c(\nu)$  determined from the observation, we have  $H \simeq 16 \text{ gauss}$  and  $N_0 = 7.8 \times 10^2$ . We can then determine  $\nu_{\text{max}}$  from these parameters to be  $4 \times 10^{11} \text{ c/s}$ , which is consistent with the restriction  $10^{11} \text{ c/s} \lesssim \nu_{\text{max}} < 10^{12} \text{ c/s}$ .

### § 5. Conclusions and discussion

We have interpreted the infrared and the optical continuum radiation of 3C 273 by an ensemble of relativistic electrons as follows. We consider a source which contains relativistic electrons and magnetic fields, and which is optically thick to the radio radiation. Assuming that the steep decrease of the spectral power with increasing frequency in the infrared is due to the upper cutoff of the synchrotron radiation and that  $\beta = 1$ , we can interpret the flat optical continuum to be produced by the inverse Compton process. The same interpretation can essentially be applied for other quasars and possibly some of the Seyfert-type nuclei high frequency parts of whose optical continuum spectra have flat slopes. It must be remarked that the spectral shape in the infrared may not necessarily be the same for these objects owing to the following reason. The energy spectrum of relativistic electrons which is, for simplicity, cut off completely at  $\gamma_2$  in our treatment may not be valid strictly. It is probable that the energy spectra have certain kinds of high energy tails which are nicely distinct each other, so that the resultant spectral shapes of the synchrotron radiation may also show small differences.

We have determined the source parameters of 3C 273 under the present interpretation. Two extremes are then required, one is the presence of large magnetic fields of the order of 100 gauss and the other is quite a short life-time of energetic electrons of the order of 10 seconds. According to Syrovatskii, the rapid acceleration of particles can occur in a region near a neutral line of the magnetic fields, which may be produced by the turbulent motions of magnetized gas clouds.<sup>21),22)</sup> Although it is difficult without the precise model of the source to show that the relativistic electrons with required energy is really produced in a time scale of the order of 10 seconds, the acceleration mechanism suggested by Syrovatskii may give a theoretical ground to our interpretation.

### Acknowledgements

The author would like to express his sincere thanks to Professor C. Hayashi for encouraging discussions, and to Professor K. Kawabata for helpful discussions and reading the manuscript.

### Appendix

The production rate of the inverse Compton photons is calculated for a  $\nu_{\max}$ , which is in the present treatment limited by  $\nu_{\max} \ll \nu_2$ , as follows.

Using Eqs. (1) and (7) in the paper, we define  $F(\nu)$  and  $G(\nu)$  as functions of  $\nu$ ,

$$F(\nu) \equiv \int_{r_1}^{r_2} N(r) \sigma(\nu', \nu, r) dr,$$

$$G(\nu) \equiv \int_{(\nu'/4\nu)^{1/2}}^{r_2} N(r) \sigma(\nu', \nu, r) dr.$$

The spectral number density of the synchrotron photons given by Eq. (6) is now rewritten as

$$n_s(\nu) d\nu = \begin{cases} n_{s1}(\nu) d\nu & \text{for } \nu \leq \nu_{\max}, \\ n_{s2}(\nu) d\nu & \text{for } \nu \geq \nu_{\max}. \end{cases}$$

Using  $F(\nu)$ ,  $G(\nu)$  and  $n_s(\nu)$ , we further define the following four quantities,

$$F1(\nu) = c \int F(\nu) n_{s1}(\nu) d\nu,$$

$$F2(\nu) = c \int F(\nu) n_{s2}(\nu) d\nu,$$

$$G1(\nu) = c \int G(\nu) n_{s1}(\nu) d\nu,$$

$$G2(\nu) = c \int G(\nu) n_{s2}(\nu) d\nu.$$

As in the case of the thin source, we can obtain the production rate of the inverse Compton photons,  $n_c(\nu') d\nu'$ , as follows. For the frequency range  $\nu_1 \leq \nu \leq \nu_1 \gamma_1^2$ ,

if  $\nu' \leq \nu_{\max}$ ,  $n_c(\nu') d\nu' = F1(\nu') - F1(\nu_1)$ ,

if  $\nu' \geq \nu_{\max}$ ,  $n_c(\nu') d\nu' = F1(\nu_{\max}) - F1(\nu_1) + F2(\nu') - F2(\nu_{\max})$ .

For  $4\nu_1 \gamma_1^2 \leq \nu' \leq \nu_2$ ,

if  $\nu' \geq 4\gamma_1^2 \nu_{\max}$ ,

$$n_c(\nu') d\nu' = G1(\nu_{\max}) - G1(\nu_1) + G2(\nu'/4\gamma_1^2) - G2(\nu_{\max}) + F2(\nu') - F2(\nu'/4\gamma_1^2),$$

if  $\nu_{\max} \leq \nu' \leq 4\gamma_1^2 \nu_{\max}$ ,

$$n_c(\nu') d\nu' = G1(\nu'/4\gamma_1^2) - G1(\nu_1) + F1(\nu_{\max}) - F1(\nu'/4\gamma_1^2) + F2(\nu') - F2(\nu_{\max}),$$

if  $\nu' \leq \nu_{\max}$ ,

$$n_c(\nu') d\nu' = G1(\nu'/4\gamma_1^2) - G1(\nu_1) + F1(\nu') - F1(\nu'/4\gamma_1^2).$$

For  $\nu_2 \leq \nu' \leq 4\nu_2 \gamma_1^2 (= 4\nu_1 \gamma_2^2)$ ,

if  $\nu' \geq 4\gamma_1^2 \nu_{\max}$ ,

$$n_c(\nu') d\nu' = F2(\nu_2) - F2(\nu'/4\gamma_1^2) + G1(\nu_{\max}) - G1(\nu_1) + G2(\nu'/4\gamma_1^2) - G2(\nu_{\max}),$$

if  $\nu' \leq 4\gamma_1^2 \nu_{\max}$ ,

$$n_c(\nu') d\nu' = F1(\nu_{\max}) - F1(\nu'/4\gamma_1^2) + F2(\nu_2) - F2(\nu_{\max}) + G1(\nu'/4\gamma_1^2) - G1(\nu_1).$$

For  $4\gamma_1^2 \nu_2 \leq \nu' \leq 4\gamma_2^2 \nu_2$ ,

if  $\nu' \geq 4\gamma_2^2 \nu_{\max}$ ,

$$n_c(\nu') d\nu' = G2(\nu_2) - G2(\nu'/4\gamma_2^2),$$

if  $\nu' \leq 4\gamma_2^2 \nu_{\max}$ ,

$$n_c(\nu') d\nu' = G1(\nu_{\max}) - G1(\nu'/4\gamma_2^2) + G2(\nu_2) - G2(\nu_{\max}).$$

### References

- 1) F. J. Low and D. E. Kleinmann, *Astron. J.* **73** (1968), 868.
- 2) A. G. Pacholczyk and R. J. Weymann, *Astron. J.* **73** (1968), 870.
- 3) K. Takarada, *Prog. Theor. Phys.* **40** (1968), 770.
- 4) K. I. Kellermann, B. G. Clark, C. C. Bare, O. Rydbleck, J. Ellder, B. Hansson, E. Kollberg, B. Hoglund, M. H. Cohen and D. L. Jauncey, *Astrophys. J.* **153** (1968), L209.
- 5) J. M. Hornby and P. J. S. Williams, *Month. Notices Roy. Astron. Soc.* **131** (1966), 237.
- 6) P. A. G. Scheur, *Plasma Astrophysics* (Academic Press, New York and London, 1967), p.262.
- 7) J. B. Oke and W. L. W. Sargent, *Astrophys. J.* **151** (1968), 807.
- 8) J. B. Oke, W. L. W. Sargent, G. Neugebauer and E. E. Becklin, *Astrophys. J.* **150** (1967), L173.
- 9) V. L. Ginzburg and S. I. Syrovatskii, *Ann. Rev. Astron. Astrophys.* **3** (1965), 297.
- 10) J. E. Felten and P. Morrison, *Astrophys. J.* **146** (1966), 686.

- 11) V. L. Ginzburg and S. I. Syrovatskii, *Soviet Phys.—JETP* **19** (1964), 1255.
- 12) W. E. Baylis, W. M. Schmid and E. Luscher, *Z. Astrophys.* **66** (1967), 271.
- 13) J. B. Oke, *Astrophys. J.* **141** (1965), 6.
- 14) F. J. Low and H. L. Johnson, *Astrophys. J.* **141** (1965), 336.
- 15) K. I. Kellermann and I. I. K. Pauliny-Toth, *Ann. Rev. Astron. Astrophys.* **6** (1968), 417.
- 16) W. A. Dent, *Astrophys. J.* **153** (1968), L29.
- 17) E. E. Epstein, *Astrophys. J.* **142** (1965), 1285.
- 18) F. J. Low, *Astrophys. J.* **142** (1965), 1287.
- 19) E. T. Byram, T. A. Chubb and H. Friedman, *Science* **152** (1966), 66.
- 20) J. B. Oke, *Astrophys. J.* **147** (1967), 901.
- 21) S. I. Syrovatskii, *Soviet Astron.—AJ* **10** (1966), 270.
- 22) E. Schatzman, *Astron. J.* **73** (1968), 909.
- 23) T. D. Kinman, *Astron. J.* **73** (1968), 885.